geographies

MDPI

Article

Mapping Built-Environment Exposure to Night-Time Road Traffic Noise in Malta

Ricardo Mendes Correia [1,2,*], Jorge Rocha [3] and Mario V. Balzan [1]

[1] EcoStack Innovations Limited, the Hub Workspace, Triq San Andrija, SGN 1612 San Ġwann, Malta; mario.balzan@ecostackinnovations.com
[2] Centre for Research in Anthropology (CRIA), Iscte-Instituto Universitário de Lisboa, Av. Das Forças Armadas 40, 1649-026 Lisboa, Portugal
[3] Institute of Geography and Spatial Planning (IGOT), Universidade de Lisboa, Rua Branca Edmée Marques, 1600-276 Lisboa, Portugal; jorge.rocha@edu.ulisboa.pt
* Correspondence: ricardo.mendes.correia@iscte-iul.pt

Abstract

Strategic noise maps support environmental policy but may obscure how exposure relates to the built environment, socioeconomic conditions and road network structure. This study integrates Malta's 2021 night-time road traffic noise contours with 142,681 building footprints, local council socioeconomic indicators and a road network derived from a historical OpenStreetMap snapshot. Of the building footprints, 13,773 (9.65%) intersected contours at or above 50 dB, representing 1.92 km^2 (6.26%) of the national building-footprint area. Socioeconomic disadvantage showed no strong monotonic relationship with exposure across 68 local councils, although higher noise exposure was concentrated in a subset of disadvantaged localities. At 500 m, the road length in the top centrality decile was associated with the exposed building count (Spearman $\rho = 0.614$) and footprint share ($\rho = 0.604$). Priority screening identified 23 cells in 15 clusters where high road centrality coincided with a greater mapped building-footprint area in higher noise classes. The results show how strategic noise mapping can support more targeted environmental action by identifying administrative divisions (local councils) where socioeconomic disadvantage coincides with higher levels of noise exposure and transport corridors where greater building exposure overlaps with structurally important roads.

Keywords: road traffic noise; strategic noise mapping; building exposure; road-network centrality; environmental inequality; Malta

Check for updates

Academic Editor: Aleksandar Stevanovic

Received: 24 September 2026
Revised: 2 November 2026
Accepted: 4 November 2026
Published: 9 November 2026

Copyright: © 2026 by the authors. Licensee MDPI, Basel, Switzerland. This article is an open access article distributed under the terms and conditions of the Creative Commons Attribution (CC BY) license.

1. Introduction

Environmental noise is a widespread pressure associated with transport systems and a major concern for public health and urban policy. Road traffic represents the main source of transport-related noise exposure across much of Europe, contributing to adverse outcomes including annoyance, sleep disturbance and cardiovascular and metabolic effects [1,2]. Its spatial distribution is closely related to both transport infrastructure and the morphology of urban settlements, making road traffic noise simultaneously an environmental, transport and planning issue.

Night-time exposure is particularly relevant because of its relationship with sleep disturbance and cumulative long-term exposure. The World Health Organization recommends reducing road traffic noise during the night to below 45 dB Lnight [1]. Within the European regulatory framework, however, reporting obligations applicable to strategic planning begin

at higher thresholds. Directive 2002/49/EC established Lden and Lnight as common indicators for strategic noise mapping and requires Member States to assess major environmental noise sources and develop corresponding action plans [3]. Subsequent development of the Common Noise Assessment Methods in Europe (CNOSSOS-EU) further harmonised calculation procedures for road, railway, aircraft and industrial noise [4,5].

Strategic noise maps consequently constitute an important harmonised spatial evidence base, but their regulatory purpose may condition what they represent. Published classes do not provide a continuous description of all environmental noise across a territory. In particular, locations outside reported Lnight ≥50 dB polygons cannot automatically be interpreted as experiencing less than 50 dB because lower road noise levels, roads outside the scope of strategic mapping and other environmental noise sources may still be present. This distinction becomes important when regulatory datasets are reused for secondary spatial analysis.

Geographic Information Systems offer considerable potential to extend strategic noise mapping beyond the aggregate presentation of results by integrating acoustic information with physical receptors and other spatial datasets [6]. GIS-based environmental noise studies have combined noise maps with buildings, population and other receptor information, allowing exposure to be analysed at finer spatial resolutions than administrative totals alone provide [7–9]. Recent work has also sought to extend strategic noise maps towards more operational representations of road traffic noise. Puyana-Romero et al. [10] developed a GIS-based approach to identify and prioritise noise hotspots associated with major roads, while Baclet et al. [11] introduced receiver-centric noise-exposure sensitivity mapping to support network-level assessment.

Building geometry provides a particularly useful representation of the physical environment. Exposure can be characterised not only by the number of structures intersecting a mapped noise class but also by the amount of building-footprint area contained within that class. The two indicators need not produce the same geographical pattern. Areas containing numerous small, affected buildings can differ markedly from areas where fewer but larger structures contribute a substantial quantity of exposed built fabric.

In addition to territorial differences, the socioeconomic distribution of environmental noise merits examination. Evidence from the WHO European Region shows mixed relationships between socioeconomic position and environmental noise exposure, although deprivation measures more often identify higher exposure among lower socioeconomic groups and small-area analyses remain comparatively limited [12]. This motivates testing whether differences among Malta's local councils are only territorial or are also socioeconomically patterned while maintaining the distinction between area-level conditions and individual exposure.

The spatial organisation of road traffic noise can also be considered in relation to the road network through which its principal source operates. Road systems are structurally heterogeneous: individual segments differ in connectivity and in their position relative to the rest of the network. Graph theory provides a formal framework for representing these relationships [13], and measures such as degree, closeness and betweenness centrality have become established tools for analysing urban street structure [14–18].

Betweenness is particularly useful for identifying network elements occupying important positions on shortest paths. Applications to urban street networks have demonstrated relationships between network structure and the distribution of land uses, services and urban activities [19–21]. Previous network-constrained spatial research has also demonstrated the analytical value of examining urban phenomena along street systems rather than exclusively in unrestricted Euclidean space [22]. More broadly, graph centrality, accessibil-

ity and spatial intensity can be understood as related but conceptually distinct dimensions of urban spatial organisation [23–25].

Previous studies have related road traffic noise to urban form and to road-network characteristics using indicators such as road-network density, road-area density, road geometry, junction configuration and local street structure [26–29]. These studies demonstrate that road-network structure is relevant to the spatial distribution of traffic noise but address different analytical relationships from that examined here. The spatial correspondence between building exposure represented in statutory Lnight products and the topological importance of the road network remains comparatively underexplored, particularly when exposure is derived from building-footprint intersections and examined across multiple spatial supports.

That distinction is central to the present study. Structural road-network centrality does not represent observed traffic flow and should not be treated as a substitute for vehicle counts, speed, congestion or acoustic emissions. Rather, it describes the positional importance of a road segment within the wider network. Combining strategic noise mapping and network analysis therefore creates a complementary analytical perspective: strategic Lnight contours describe where modelled acoustic exposure occurs, whereas network centrality identifies road segments occupying structurally important positions in the transport system. Their spatial coincidence does not establish that centrality causes acoustic exposure, but it can identify locations where substantial built-environment exposure and network importance converge.

Malta provides an appropriate setting for examining these relationships. Environmental and road traffic noise have been investigated previously in the Maltese Islands. Earlier studies investigated environmental noise assessment and road traffic noise control procedures [30], local traffic noise conditions around the Mriehel bypass [31], the wider spatial distribution of environmental noise across the Maltese Islands [32], and noise and vibration associated with major infrastructure proposals such as the Kappara Junction project [33]. These studies established the relevance of road traffic as an environmental noise source in Malta, but they largely preceded the current Round-4 strategic noise dataset and did not integrate national building geometry with structural road-network analysis.

Malta's fourth round of strategic noise mapping uses 2021 as its assessment reference and applies the END/CNOSSOS-EU framework to major-road sources and relevant roads within the designated agglomeration [34]. The associated major-road inventory extends to approximately 354.9 km. The availability of harmonised Lnight vector contours through the European infrastructure used for environmental data reporting consequently creates the opportunity to analyse, at national scale, the spatial relationship between officially modelled road noise and Malta's built environment.

A remaining challenge is to integrate statutory acoustic outputs, building-footprint exposure and structural road-network centrality within a common spatial framework while also considering the socioeconomic context of territorial differences. Strategic noise maps identify the spatial distribution of modelled noise bands but do not quantify the proportion of individual building footprints affected, differences in exposure or how exposure varies among local councils. They also do not show whether these territorial differences are associated with socioeconomic conditions or where higher building exposure coincides with structurally important transport corridors. Conversely, conventional network-centrality analysis describes the structure of the transport network without accounting for the environmental exposure of the surrounding built fabric.

The purpose of this study is to assess how the physical built environment represented in Malta's statutory 2021 night-time road-noise maps is distributed across buildings and local councils and whether it coincides with socioeconomic disadvantage or structurally im-

portant roads. It brings together four complementary outputs: class-specific and fractional building-footprint intersections; local council exposure and socioeconomic profiles; descriptive associations with road-network centrality across spatial scales; and joint screening of higher-noise building-footprint areas and road centrality. The contribution is a reproducible spatial screening framework using published strategic-noise products, not a new acoustic model, traffic-flow prediction or individual-exposure estimate or a claim that network centrality causes noise. These outputs are intended to help identify localities and corridors for subsequent receptor-based acoustic and transport assessment rather than prescribe mitigation measures from spatial overlap alone.

The analysis is organised around four research questions:

1. How much of Malta's physical building stock and building-footprint area intersects the officially mapped road traffic Lnight classes, and how is that exposure distributed among noise bands?
2. How is mapped built-environment exposure distributed across local councils with different socioeconomic profiles, and are higher levels of road traffic noise exposure concentrated in more disadvantaged localities?
3. To what extent is building exposure spatially associated with structurally important parts of the road network, and is the relationship consistent across alternative spatial aggregation scales?
4. Which locations combine high structural road-network centrality with substantial building-footprint exposure to higher Lnight classes?

2. Study Area and Data

2.1. Study Area and Temporal Framework

The study covers the Maltese Islands at national scale, using the 68 local councils as the principal administrative units for sub-national comparison. The acoustic component corresponds to the 2021 assessment year of Malta's fourth round of strategic noise mapping. The same year was used for population contextualisation through the 2021 Census of Population and Housing. For network analysis, an OpenStreetMap snapshot from 1 January 2022 was selected to minimise temporal mismatch with the acoustic assessment.

The analysis should therefore be interpreted as a spatial assessment centred on 2021 environmental noise conditions and not as an assessment of noise conditions in 2026. Later dates associated with data access or European publication refer to dissemination rather than to the acoustic reference year.

2.2. Strategic Road-Noise Data

The principal acoustic dataset corresponded to the consolidated Round-4 Environmental Noise Directive dataset made available through the EEA/Reportnet system [35]. The analysis used the Malta layer NoiseContours_majorRoadsIncludingAgglomeration_Lnight, which represents the officially reported night-time road-traffic noise contours for the 2021 assessment year. These published polygons represent modelled strategic mapping bands. Their intersection with a horizontal building footprint does not determine noise at a façade receptor: façade exposure additionally depends on receiver height, orientation, screening, the distribution of acoustic energy around the building and the spatial resolution of the modelled noise field. The mapped area of an intersected footprint is therefore used only as a physical spatial screening indicator.

The layer contained 481 MultiPolygon features in ETRS89-LAEA Europe (EPSG:3035), distributed among five reported Lnight classes: 50–54, 55–59, 60–64, 65–69 and ≥70 dB. There were 143 polygons in the 50–54 dB class, 79 in 55–59 dB, 125 in 60–64 dB, 84 in 65–69 dB and 50 in the ≥70 dB class. The total geometrical area of the published vector contours

was approximately 26.52 km^2. A comparison between classes identified approximately 15 m^2 of residual overlap, which appears to result from boundary or sliver artefacts. The rules used to allocate these areas still require verification against the original overlay scripts.

The analysis uses the published vector contours themselves. It does not attempt to reconstruct the underlying acoustic surfaces or reproduce the SoundPLAN/CNOSSOS-EU modelling process. A difference was identified between the vector area calculated directly from the disseminated polygons and the rounded noise-class areas reported in the Malta Round-4 technical documentation [34]. No rescaling or reconstruction was introduced to reconcile these values because doing so would modify the officially disseminated spatial product. Locations outside the published polygons were therefore classified as 'Outside mapped ≥50 dB contours', rather than as Lnight <50 dB.

2.3. Building Footprints and Administrative Boundaries

Building footprints were obtained from the Malta Planning Authority's Large Scale Topography Buildings WFS [36]. The initial retrieval using conventional pagination returned 142,681 records but only 90,990 distinct non-empty source identifiers, corresponding to 51,691 repeated records. This retrieval was therefore not used as the analytical source. The subsequent acquisition used spatial bounding boxes subdivided recursively into tiles. Reported WFS feature counts were checked, and duplicate records at tile boundaries were removed using the stable GML source identifier. The resulting dataset contained 142,681 distinct source identifiers. An independent audit of the raw BBOX file and the final building exposure GeoPackage confirmed that neither contained duplicate identifier pairs. All 142,681 final building geometries are valid, including 11 with multiple polygon parts. The analytical unit is an official building polygon feature, not necessarily an occupied dwelling or a single functional building. Areas were calculated in EPSG:3035, giving a total footprint area of 30.6423 km^2. The source code, derived outputs and independent audit specifications were provided in a separate computational archive for editorial and peer review assessment.

The full physical building dataset was retained. No attempt was made to identify residential buildings or dwellings because the study concerns the physical built environment rather than household or person-level exposure. Local council boundaries were obtained from the official national administrative dataset. Selection of administrative level 5 produced 68 local council polygons, which were validated and transformed to EPSG:3035 [37].

2.4. Population and Socioeconomic Data

Population information was derived from the 2021 Census of Population and Housing produced by the National Statistics Office of Malta [38]. The 68 local council counts summed to a national usual-resident population of 519,562.

Population was retained exclusively as a local council-level contextual variable. It was not redistributed to buildings, addresses or façade receptors. Population-normalised indicators therefore describe the scale of physical building exposure relative to local council population and should not, consequently, be interpreted as estimates of individual noise exposure.

Additional locality-level socioeconomic indicators were obtained from the 2021 Census dwelling, education and employment volumes. Three variables were retained to represent complementary dimensions of disadvantage: the percentage of residents aged 10 years or over classified as illiterate; the share of unemployed persons among employed plus unemployed residents aged 15 years or over; and the percentage of main residential dwellings needing serious repairs or classified as dilapidated [39,40]. These variables provide educational, labour market and housing condition descriptors at local council level and are not individual level characteristics.

2.5. Road Data

Two complementary road datasets were used because statutory road-noise mapping and structural network analysis require distinct spatial representations. The official Round-4 DF1_5 major-road source dataset contained 8415 reported source segments, with a combined reported length of approximately 354.912 km, together with annual traffic-flow information and source identifiers. This dataset was used to characterise the official road-source information and to validate the strategic noise-mapping context.

Because the distributed table did not provide the complete connected geometry required for national graph analysis, road centrality was calculated from a historical OpenStreetMap dataset distributed by Geofabrik [41,42]. The selected snapshot dated 1 January 2022 contained 30,311 original LineString road features. For graph construction, trunk, primary, secondary and tertiary roads and associated link classes were retained, together with unclassified roads, residential roads and living streets. Service roads, tracks, footways, paths, pedestrian ways, steps and cycleways were excluded. The filtering produced 15,639 source road features. Road geometries were transformed to ETRS89/UTM zone 33N (EPSG:25833) before graph construction so that edge lengths and shortest-path distances could be expressed metrically (Table 1).

Table 1. Principal datasets used in the analysis.

Dataset	Source	Temporal Reference	Representation	Analytical Role
Round-4 road traffic Lnight contours	EEA/Reportnet; ERA	2021	481 polygons	Official strategic noise exposure
Buildings	Planning Authority	National dataset	142,681 footprints	Physical built-environment exposure
Local councils	Planning Authority/Malta Data Portal	Administrative boundaries	68 polygons	Territorial aggregation
Census population and socioeconomic indicators	NSO Malta	2021	Local council counts and rates	Population context; socioeconomic inequality
END DF1_5 roads	EEA/Reportnet	Round 4	8415 source segments; 354.912 km	Official road-source metadata
Historical road network	OSM/Geofabrik	1 Jan 2022	15,639 retained roads	Structural network analysis

3. Methods

3.1. Analytical Framework

The workflow combined established GIS-based environmental noise exposure assessment with graph-based road-network analysis. The analysis comprised seven main stages: preparation and quality control of the spatial datasets; building-level Lnight overlay; local council aggregation and population contextualisation; socioeconomic inequality analysis; sensitivity testing; construction and analysis of the road graph; and multi-scale integration of building exposure with structural road centrality.

The principal outcome is physical built-environment exposure. The study does not estimate the number of residents exposed to noise.

3.2. Building-Level Lnight Exposure

For each building-footprint polygon b and mapped noise class c, the intersected area was defined by the equation below. The original processing retained an intersection only when its calculated area was strictly greater than 0.01 m^2. Smaller intersections and numerical contacts were excluded. The operational condition is therefore >0.01 m^2, not ≥0.01 m^2.

$$A(b,c) = \text{Area}(B(b) \cap N(c))$$

Areas intersecting each noise class were calculated from the published polygons and summed to obtain the mapped building-footprint area. For counts, each building polygon was assigned to only its highest qualifying class, preventing duplicate building counts. However, the original area calculation did not remove overlap between noise classes before summation. An independent union audit of all 481 valid contour polygons identified 12.72 m^2 of overlap between classes, with no detectable overlap within the same class. This is the maximum possible area counted more than once across the building footprints and represents less than 0.0007% of the approximately 1.917 km^2 of the reported mapped footprint area. In the building table, 38 features had a summed mapped area slightly greater than their total footprint area. The combined excess was 0.0223 m^2. The reported area is therefore the sum of the intersections with individual classes, including a measured but very small overlap artefact. It is not presented as an exact geometric union at sub square metre precision.

3.3. Local Council Aggregation and Population Context

Each building was assigned to one local council using an interior representative point. Five of the 142,681 building features fell outside the local council polygons; their combined footprint area was approximately 63.9 m^2, and none intersected the mapped ≥50 dB noise contours. They therefore had no effect on local council exposure totals.

For each local council, three principal exposure dimensions were calculated: the number of buildings intersecting mapped contours; the proportion of the local council's building stock intersected; and the proportion of the total building-footprint area within the mapped contours. Counts and areas were also calculated for the ≥60 and ≥65 dB classes. Population-normalised indicators, including exposed buildings per 1000 residents and exposed footprint area per resident, were calculated as secondary contextual descriptors. Population was not allocated to individual buildings because the available census data were aggregated at local council level. This option avoids inferring individual characteristics from relationships identified in aggregate data, the classic problem discussed by Robinson [43]. It also follows the methodological caution normally associated with ecological studies, according to which aggregate data should not be used as substitutes for individual information [44]. Consequently, population-normalised indicators were used only as contextual descriptors and not as estimates of individual exposure.

3.4. Socioeconomic Inequality Indicators

Socioeconomic inequalities were examined at local council level using an exploratory socioeconomic disadvantage index (SDI). The three Census 2021 inputs represent different denominators and dimensions: illiterate residents as a percentage of the population aged 10 years or over; unemployed persons divided by employed plus unemployed residents aged 15 years or over; and main residential dwellings needing serious repairs or classified as dilapidated divided by all main residential dwellings [39,40]. Higher values consistently denote greater disadvantages. The three percentages were not added directly: for each indicator x and council i, $z_i = (x_i - \text{mean}(x))/\text{SD_population}(x)$, using the unweighted mean and population standard deviation across the 68 councils. The SDI is the equally

weighted arithmetic mean of the three z scores. Equal weights were chosen to retain a transparent summary of education, labour market and housing condition disadvantage rather than imply that a statistically calibrated latent deprivation scale was identified. The components need not be interchangeable and may reflect differences in age structure or building age. All 68 councils had values for these indicators. The standardisation parameters, original inputs and computed scores are given in Supplementary Tables S1 and S4. This index is not an official Maltese deprivation index.

The observed intercorrelations among the three SDI dimensions were modest: Spearman $\rho = 0.116$ for illiteracy versus unemployment, $\rho = 0.351$ for illiteracy versus poor housing condition, and $\rho = 0.328$ for unemployment versus poor housing condition (all $n = 68$; Supplementary Table S3). These components therefore describe related but non-identical dimensions. Their equal contribution is a transparent modelling choice, not evidence of a validated single latent scale.

Spearman's rank correlation compared the SDI with six council-level indicators: percentages of building features and of the total building-footprint area intersecting mapped ≥50, ≥60 and ≥65 dB classes. The primary specification used all 68 councils without missing-value exclusions. Alternative specifications examined each of the three components separately, the mean of the three within-sample percentile ranks, and three two-component indices obtained by omitting one component at a time. The percentile-rank index averages each indicator's ascending rank divided by the number of eligible councils, with higher values indicating greater disadvantage; sample-restricted indices are restandardised within their respective samples. The sensitivity samples exclude Mdina (n = 67) or retain councils with at least 2000 inhabitants (n = 60). The full set of coefficients and sample sizes, including the six primary specifications and sensitivity checks, is provided in Supplementary Table S2. Councils were also grouped by SDI quintile and screened for joint upper-quintile SDI and ≥60 dB exposed footprint share. These are area-level descriptive comparisons, not estimates of individual socioeconomic gradients.

3.5. Sensitivity to Marginal Contour Intersections

The primary classification considered a building to intersect a published Lnight class when the footprint intersection was strictly greater than 0.01 m^2. Smaller contacts were excluded as geometric artefacts, as described in Section 3.2. Class assignments were then repeated using minimum intersections of 1%, 5%, 10%, 25% and 50% of each building polygon's total footprint. For each threshold, the highest class meeting the specified proportion was retained. These thresholds test the influence of marginal geometric intersections. They are not statutory or health-based exposure thresholds and do not assess uncertainty in the acoustic model or positional errors in the published contour boundaries.

3.6. Road-Network Construction

Network analysis follows established graph-based approaches to urban street structure [13,16–18]. Previous work by Correia et al. [22] similarly represented urban streets as a finite network and used shortest-path distance for network-constrained spatial analysis. The present study extends this general analytical perspective to structural road centrality.

Every consecutive road-geometry vertex was retained to preserve metric road length and curvature. The network was modelled as undirected and length weighted because the objective was to characterise structural through-movement potential rather than simulate operational traffic assignment. The resulting graph contained 79,281 geometry nodes and 87,322 edges, representing approximately 2366.9 km of filtered road network.

3.7. Structural Edge-Betweenness Centrality

Structural importance was measured using edge-betweenness centrality [14,15,45]. For an edge e, betweenness is the sum, across origin-destination pairs, of the proportion of shortest paths passing through that edge. Shortest paths were weighted by metric road length:

$$C_B(e) = \Sigma_(s \neq t) \left[\sigma_st(e)/\sigma_st\right]$$

A modification was introduced to reduce sensitivity to road digitisation density. All geometry vertices remained available as intermediate shortest-path vertices, but only graph nodes with degree ≠2 were used as structural origins and destinations. These correspond mainly to junctions and dead ends rather than intermediate shape vertices. In pure-cycle components containing an insufficient number of structural nodes, all vertices were used as an alternative.

Components containing more than 500 structural nodes used a reproducible sample of 500 source nodes, selected with a fixed random seed of 42, while all structural nodes remained available as destinations. Smaller components used all structural nodes as origins and destinations. Network analysis was implemented in Python 3.14, with centrality calculated using the NetworkX 3.3 library [46]. Because raw betweenness values depend strongly on graph-component size, edge centrality was converted to percentiles calculated separately within each component. Original road features composed of several graph edges were then assigned a mean centrality percentile weighted by the length of the corresponding edges. The road graph contained 32 connected components, of which the two dominant components jointly represented approximately 99.7% of total filtered road length and were retained as the analytical core.

The robustness of the centrality estimates was assessed by repeating the analysis with samples of 250 and 1000 structural origin nodes, alternative random seeds (123 and 2026), and a configuration using all geometry vertices as origins. Compared with the original configuration of 500 origins and seed 42, Spearman rank correlations across the two main network components ranged from 0.948 to 0.986 for different sample sizes and from 0.944 to 0.955 for different seeds. The proportion of edges retained in the original highest centrality decile ranged from 90.9% to 96.3% and from 91.4% to 95.7%, respectively. When all geometry vertices were used as origins, rank correlations decreased to 0.885–0.925 and the retained proportion of upper decile edges to 81.3–89.6%. Using global rather than component specific percentile ranks also changed upper decile membership (Jaccard similarity = 0.679). The main centrality patterns therefore remained relatively stable under the sampling tests, although the selection of structural nodes and the way percentiles are calculated affect the classification of individual roads.

Structural centrality therefore describes the position of roads within the network and does not represent observed vehicle traffic.

3.8. Multi-Scale Integration of Centrality and Exposure

A common spatial support was used to combine road centrality, represented by lines, with building exposure, represented by polygons. Square grids of 250, 500 and 1000 m were generated from the same aligned origin. The 500 m grid was used for the main analysis, while the 250 and 1000 m grids allowed comparisons between scales. An independent audit also reconstructed 1000 m summaries from the archived 500 m grid by summing groups of four aligned cells and recalculating centrality weighted by road length (Table S11). Using several spatial scales reduces dependence on a single aggregation and addresses the scale component of the modifiable areal unit problem [47].

Buildings were assigned to cells using an interior representative point. Their previously calculated exact building-noise exposure attributes were then aggregated by cell. Road

geometries were clipped by grid cells, and road centrality was weighted by the length of each road portion occurring within each cell. Two network indicators were calculated: the road-length-weighted mean within-component centrality percentile and the share of road length belonging to the upper decile of structural centrality. Building indicators included exposed building counts, the exposed footprint area and percentage, and counts and footprint areas for the ≥60 and ≥65 dB classes.

The original workflow used an aligned 1 km grid origin in EPSG:25833, cell sizes of 250, 500 and 1000 m, assignment of buildings using interior points, and network indicators weighted by road length. At each resolution, the original correlation outputs distinguish three samples: cells containing roads, including those without buildings; cells containing both roads and buildings; and cells containing roads, buildings and at least one building intersecting the mapped noise contours. Their sizes were 4112/4078/1217 at 250 m, 1265/1260/493 at 500 m, and 357/356/182 at 1000 m, respectively. Correlations involving the proportion of the exposed building area exclude cells without buildings, whereas counts and absolute areas may include road cells with zero exposure. Supplementary Table S7 reports the coefficients and sample sizes for each variable and sample, and Table S13 provides the sample counts. Of the 1420 stored cells at 500 m, 1265 contained core roads, 1260 contained roads and buildings, five contained only roads, and 155 contained buildings but no core roads. Table S14 reports zero values and tied ranks for the 1260 eligible cells. These associations are descriptive because spatial dependence and possible confounding prevent ordinary iid *p*-values from being treated as confirmatory evidence.

An additional spatial dependence test used the 1260 eligible 500 m cells, binary queen adjacency [48] and 999 permutations (seed 42). Global Moran's I was 0.348 for mean structural centrality, 0.351 for the proportion of road length in the highest centrality decile, 0.311 for the proportion of exposed building footprint, 0.330 for the absolute ≥60 dB footprint area and 0.324 for the absolute ≥65 dB footprint area (Table S15). These results show spatial clustering and support the descriptive interpretation of the rank correlations. The partial rank analysis accounts for selected structural variables but does not remove spatial autocorrelation.

As a supplementary local council-scale check, the association between the proportion of road length in the highest within-component centrality decile and mapped footprint exposure was also examined after accounting for building-feature density and road-length density. Council area was calculated from administrative polygons in EPSG:3035. A partial rank correlation was calculated by residualising the average ranks of the centrality and exposure indicators against an intercept and the average ranks of building density (features/km^2) and road density (km/km^2), then correlating the two residual vectors. This descriptive analysis uses 68 local councils; it does not replace adjusted modelling within the 250, 500 or 1000 m grids and cannot control traffic volume (Supplementary Tables S6a,b).

3.9. Priority Screening

Priority screening used the 500 m cells containing both roads and buildings (n = 1260). Each cell was ranked by mean structural centrality weighted by road length and by the absolute area of the building footprint intersecting the ≥60 and ≥65 dB classes. For each variable, average ranks divided by the sample size provided a percentile score. A cell was selected when centrality and at least one of the two higher noise area indicators reached the 90th percentile. Selected cells sharing an edge or vertex were grouped. The exposure measure is the absolute affected building area, not the percentage of the total building area in the cell. It also differs from the share of road length in the highest centrality decile used for the main correlations. Recalculation using the original 500 m GeoPackage reproduced all 23 selected cells (Table S8). Alternative percentile thresholds and selection based on

exposure percentages were tested on the same cells (Table S10). This is an exploratory screening criterion, not a statutory threshold for intervention.

3.10. Software, Cartography and Reproducibility

Spatial preprocessing and cartographic quality control were carried out in QGIS 3.40.11 LTR [49]. The analytical procedures were implemented in Python using GDAL/OGR, SQLite and NetworkX. Separate scripts were used for building exposure, threshold sensitivity, road-network centrality and the combination of centrality and exposure. EPSG:3035 was used to calculate areas for noise contours, buildings and administrative polygons, while EPSG:25833 was used for metric road-network calculations. Local council exposure was mapped using Jenks natural breaks [50,51]. The publication supplement contains Figure S1 and the derived Tables S1–S15 (including S6a, S6b, S12 and S12b). The scripts and derived GIS outputs supplied separately for editorial review are not included in the publication supplement; original spatial datasets should be obtained from their respective data custodians. GDAL/OGR (https://gdal.org/; accessed on 2 November 2026) and SQLite (https://www.sqlite.org/; accessed on 2 November 2026) were used in the Python workflow; the specific GDAL/OGR and SQLite library versions were not retained in the archived processing documentation.

4. Results

4.1. National Built-Environment Exposure

The national building dataset comprised 142,681 building-footprint polygons with a combined footprint area of approximately 30.64 km^2. Of these, 13,773 buildings (9.65%) intersected at least one mapped road traffic Lnight contour ≥50 dB. The corresponding intersected building-footprint area was approximately 1.92 km^2, equivalent to 6.26% of Malta's total mapped building-footprint area (Table 2).

Table 2. National distribution of building exposure by published Lnight class.

Lnight Class	Buildings Assigned to Highest Class	% National Buildings	Intersected Footprint Area (m^2)	% Exposed Footprint Area
50–54 dB	5766	4.04	947,785	49.4
55–59 dB	4034	2.83	591,279	30.8
60–64 dB	2522	1.77	283,898	14.8
65–69 dB	1304	0.91	86,243	4.5
≥70 dB	147	0.10	8216	0.43

When classified according to the highest noise class intersecting each footprint, 5766 buildings were assigned to 50–54 dB, 4034 to 55–59 dB, 2522 to 60–64 dB, 1304 to 65–69 dB and 147 to ≥70 dB. Cumulatively, 8007 buildings (5.61%) reached a maximum intersected class of at least 55 dB, 3973 (2.78%) of at least 60 dB and 1451 (1.02%) of at least 65 dB.

The distinction between the 9.65% of buildings intersected and the 6.26% of the national building-footprint area within the contours shows that structure counts and physical built area capture different dimensions of exposure. Approximately four fifths of the total exposed footprint area occurred within the two lowest reported Lnight bands, while exposure to ≥65 and ≥70 dB was comparatively spatially restricted (Figure 1).

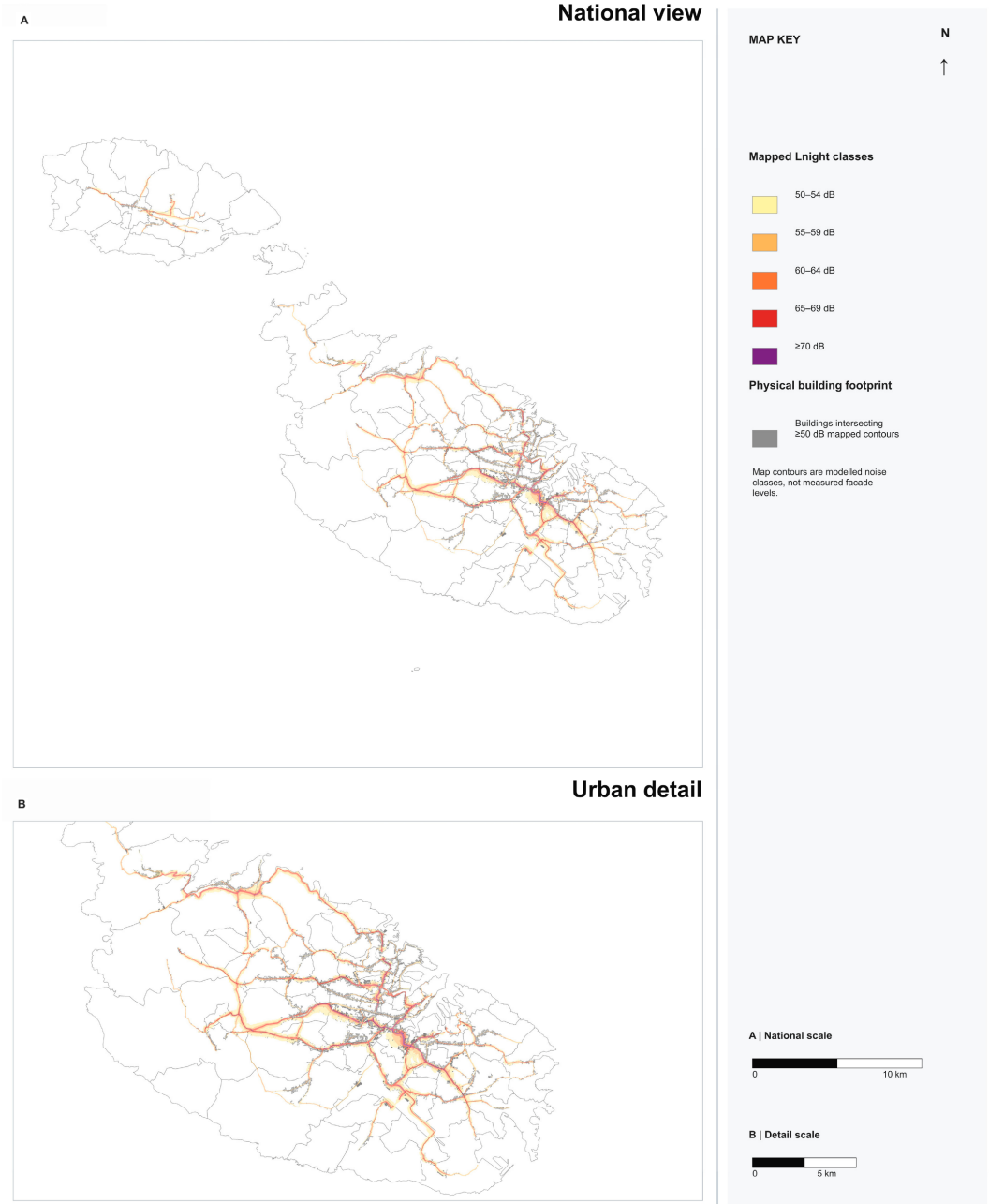


Figure 1. National distribution of night-time road traffic noise and building exposure in Malta. (**A**) National distribution of the officially reported 2021 Round-4 Lnight major-road noise classes and exposed building footprints. (**B**) Detail of the principal urbanised area. Areas outside the published contours are not interpreted as Lnight <50 dB. Scale bars are specific to each panel.

4.2. Territorial and Socioeconomic Inequalities

Exposure was strongly differentiated among Malta's 68 local councils. The highest percentages of buildings intersecting mapped ≥50 dB contours occurred in Raħal Ġdid (45.0%), Mdina (41.0%), Msida (34.2%), Marsa (34.1%) and Luqa (29.8%). Santa Luċija and Floriana each recorded approximately 27.5% (Figure 2).

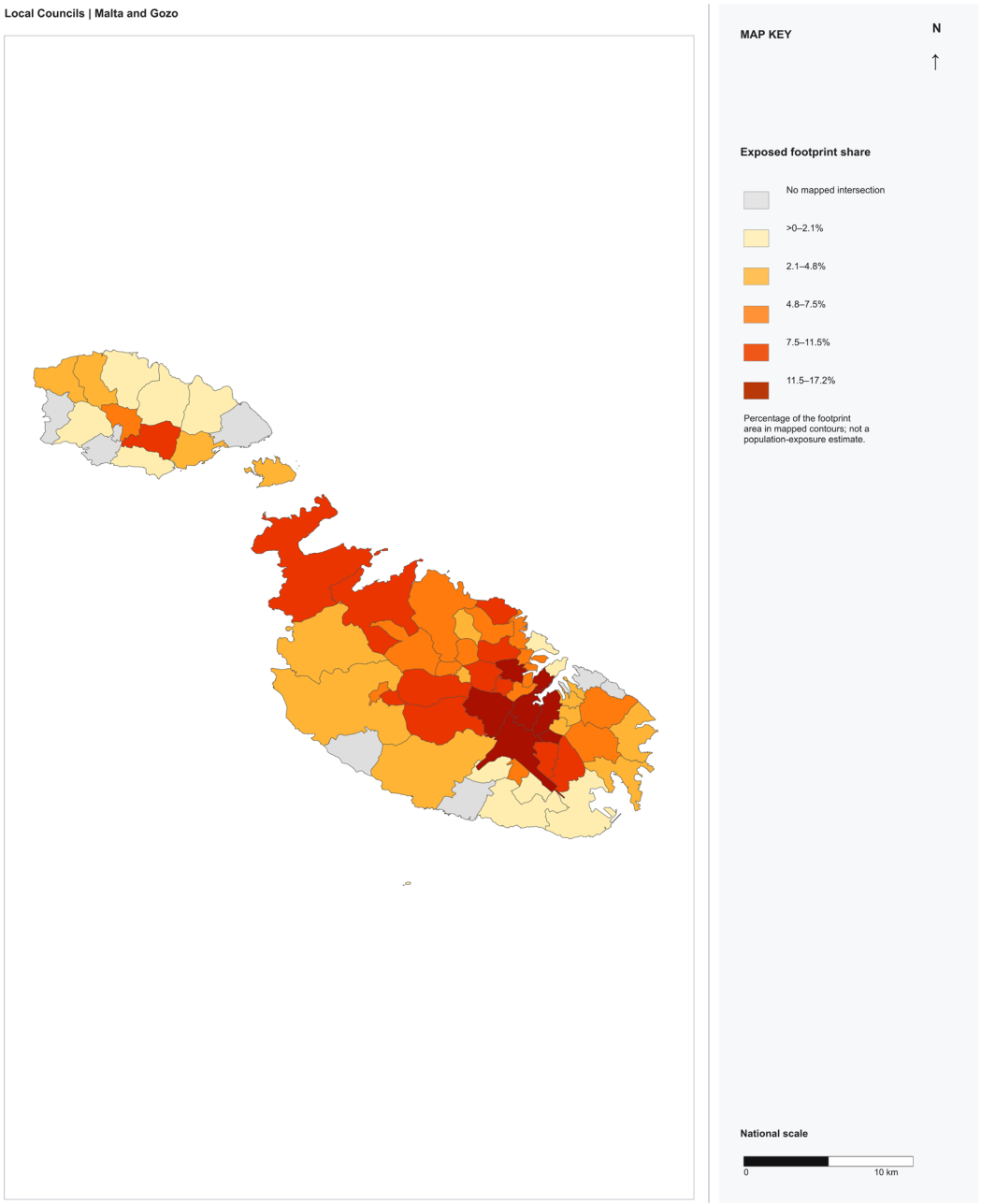


Figure 2. Territorial variation in mapped building-footprint exposure to night-time road traffic noise by local council across Malta and Gozo. Colours show the percentage of the total building-footprint area intersecting published major-road Lnight ≥50 dB contours. The map represents physical footprint exposure, not people exposed; classes use Jenks natural breaks. A single national map is displayed, including Gozo and Comino.

Absolute exposure produced a different ranking. Saint Paul's Bay contained 796 exposed buildings, followed by Qormi (753), Rahal Ġdid (721), Attard (703) and Luqa (689). Footprint-area exposure differed again. Marsa recorded the highest proportion of total building-footprint area intersecting the contours, approximately 17.2%, followed by Msida (16.8%) and Rahal Ġdid (15.0%). Santa Luċija, Luqa and Floriana recorded approximately 14.5%, 13.3% and 13.2%, respectively.

Higher noise classes were more strongly concentrated. In Marsa, approximately 16.0% of buildings reached at least 60 dB and 9.44% reached at least 65 dB. In Msida, the corresponding proportions were approximately 15.0% and 5.39%. Nine local councils, Dingli,

Fontana, Kalkara, Munxar, Qala, Qrendi, Saint Lawrence, Senglea and Xgħajra, contained no building footprint intersecting the analysed ≥50 dB contours. This absence of intersection refers exclusively to the published strategic mapping and should not be interpreted as an absence of environmental noise.

The socioeconomic extension did not identify a strong monotonic national gradient. Across all 68 local councils, Spearman coefficients for SDI against the six exposure percentages ranged from $\rho = 0.087$ to 0.180. The correlations were $\rho = 0.180$ for the percentage of building features intersecting ≥50 dB contours and $\rho = 0.117$ for the ≥60 dB exposed footprint percentage. For the latter outcome, omitting one SDI component at a time produced coefficients between 0.042 and 0.120, compared with 0.088 for the mean-of-percentile-ranks index. The coefficient was 0.096 after excluding Mdina ($n = 67$) and 0.037 for local councils with at least 2000 residents ($n = 60$). Individual SDI components also showed weak associations ($\rho = 0.020$ to 0.094 for ≥60 dB exposed footprint percentage). These tests do not support a strong or consistent monotonic national gradient. All coefficients, definitions and sample sizes are presented in Supplementary Table S2.

As an exploratory assessment of spatial dependence at local council level, global Moran's I was calculated using row-standardised queen-contiguity weights, 1999 label permutations and a fixed seed of 42. The index was $I = 0.433$ for SDI, $I = 0.350$ for ≥60 dB exposed footprint percentage and $I = 0.370$ for the percentage of building features intersecting ≥50 dB contours ($n = 68$; Supplementary Table S5). These results indicate non-negligible council-level spatial clustering and reinforce the choice not to interpret conventional independent-observation *p*-values as confirmatory. They do not constitute a spatial-dependence correction for the 250–1000 m grid correlations.

Despite these weak continuous associations, exposure was higher in the most disadvantaged quintile for several indicators. Median exposed building share was 17.10% in Q5 compared with 9.18% across Q1–Q4; the corresponding medians were 5.34% versus 2.28% for buildings reaching ≥60 dB, 1.40% versus 0.66% for ≥60 dB exposed footprint share, and 0.50% versus 0.07% for ≥65 dB exposed footprint share. The complementary road-network priority screening is illustrated in Figure 3 and discussed in Section 4.4. Seven local councils simultaneously occupied the upper quintile of SDI and the upper quintile of ≥60 dB exposed footprint share: Marsa, Raħal Ġdid, Qormi, Floriana, Luqa, Pietà and Mdina (Figure 4). The pattern therefore indicates localised concentration rather than a uniform socioeconomic gradient.

4.3. Road-Network Centrality and Exposure

The final road graph contained 79,281 geometry nodes and 87,322 edges, representing approximately 2366.9 km of road network. The two main connected components contained approximately 99.7% of filtered road length. Positive associations between structural centrality and building exposure were identified at 250, 500 and 1000 m. The accompanying road edge GeoPackage contains 87,729 line features and 32 component labels. This number of exported line features differs from the 87,322 graph edges because the source graph was constructed from rounded geometry vertices. According to the exported road layer, the two largest components represent 99.70% of filtered road length.

At the primary 500 m resolution, mean structural centrality was positively associated with the exposed building count ($\rho = 0.368$), the sensitivity-adjusted exposed building count ($\rho = 0.375$), the exposed building footprint share ($\rho = 0.383$), buildings reaching ≥60 dB ($\rho = 0.354$) and the ≥60 dB exposed footprint area ($\rho = 0.344$). Stronger associations occurred when road-network structure was represented by the share of road length belonging to the upper decile of within-component centrality.

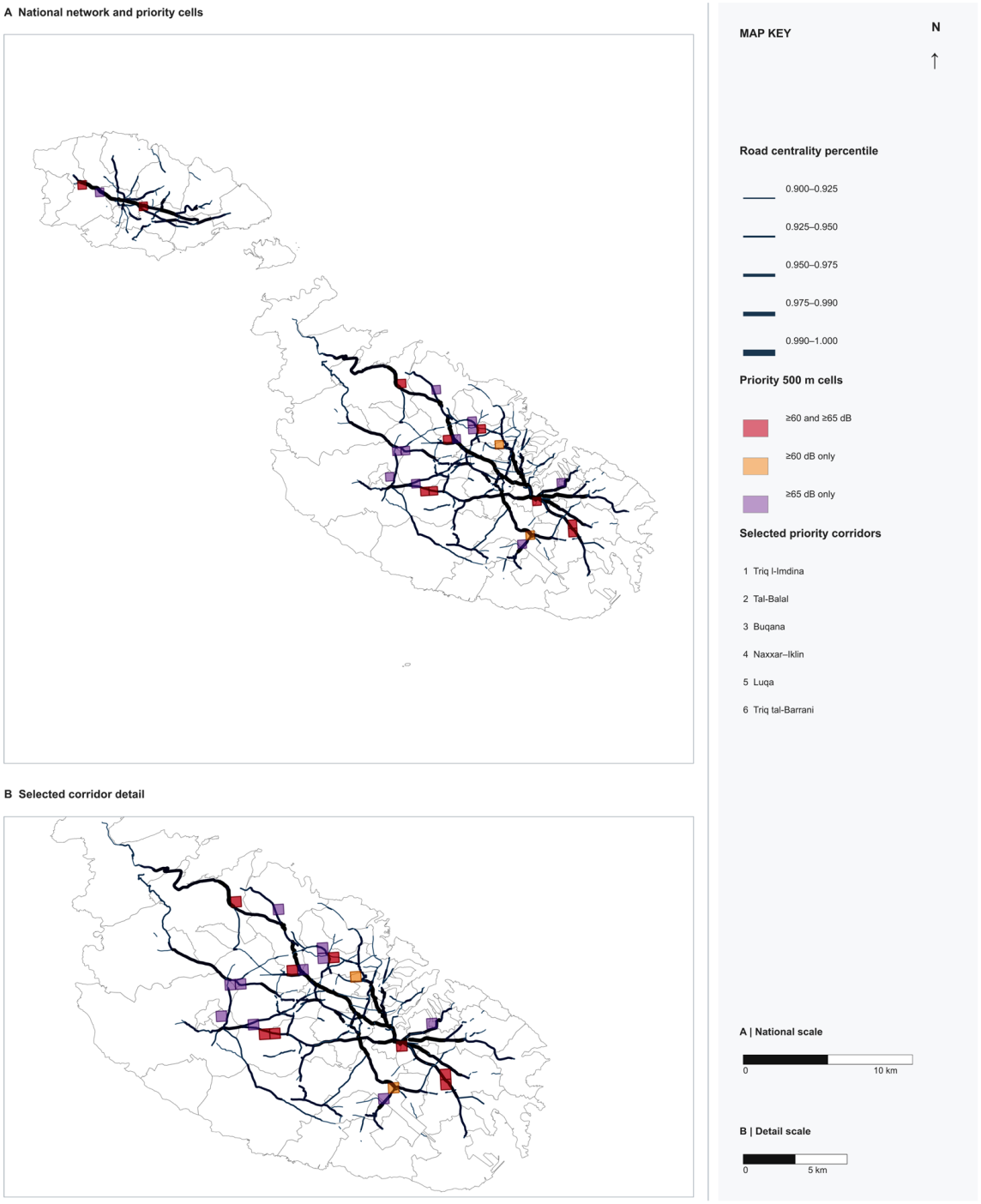


Figure 3. Structural road-network centrality and locations with higher mapped night-time noise exposure. (**A**) National distribution of roads in the highest range of structural edge-betweenness centrality calculated within each component, together with the selected 500 m cells. (**B**) Detail of the main road network in Malta. Priority cells are in the highest decile of mean structural centrality weighted by road length and in the highest decile of ≥60 and/or ≥65 dB exposed building footprint area. Each panel has its own scale bar. Supplementary Figure S1 identifies the 23 selected cells as P01–P23, corresponding to their records in Table S8.

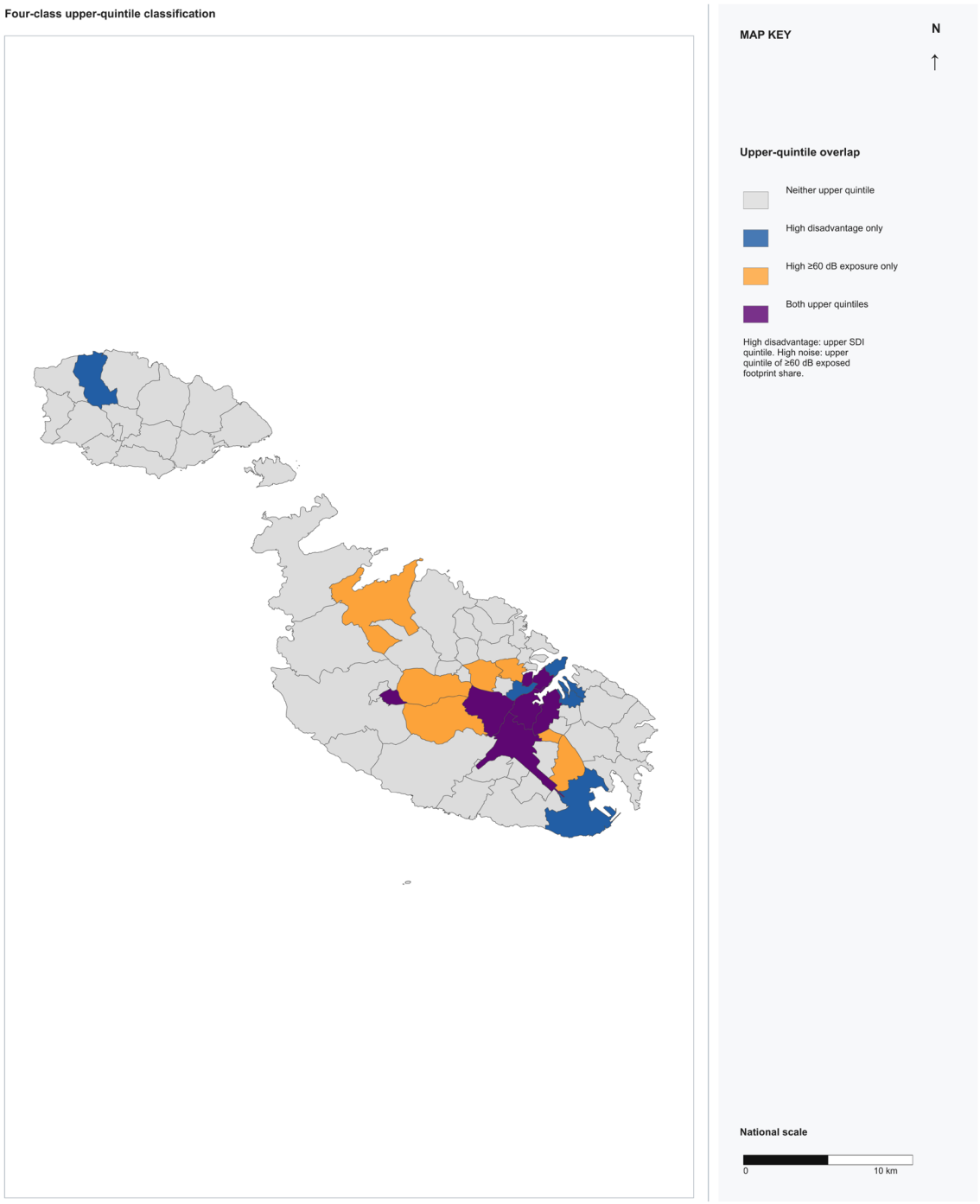


Figure 4. Socioeconomic disadvantage and higher road-noise exposure by local council. Socioeconomic disadvantage is represented by an exploratory index combining standardised locality-level illiteracy, active-population unemployment and poor housing-condition indicators. High disadvantage denotes the upper quintile of the index, and high ≥60 dB footprint exposure denotes the upper quintile of the percentage of the total building-footprint area occurring within the published Lnight classes ≥60 dB. Seven local councils occupied both upper quintiles: Marsa, Raħal Ġdid, Qormi, Floriana, Luqa, Pietà and Mdina. The classification represents ecological spatial screening and not individual exposure.

At 500 m, the share of road length in the highest centrality decile was associated with the exposed building count ($\rho = 0.614$) and the exposed building footprint share ($\rho = 0.604$). The coefficients were 0.591 for buildings reaching ≥60 dB, 0.585 for the ≥60 dB exposed footprint area, 0.516 for ≥65 dB building counts and 0.515 for the ≥65 dB footprint area.

For the exposed footprint share, the correlations were ρ = 0.509 at 250 m, 0.604 at 500 m and 0.676 at 1000 m. At local council level, the same centrality indicator was associated with ≥60 and ≥65 dB exposed footprint areas (ρ = 0.611 and ρ = 0.626, respectively). These are unadjusted associations. The higher correlations at coarser resolutions do not demonstrate an independent effect of centrality. The absolute building counts in Table 3 use cells containing roads (n = 1265), whereas the exposed footprint share uses cells containing both roads and buildings (n = 1260). Within the latter sample, the association with the exposed building count was ρ = 0.613 (Table S7).

Table 3. Association between highly central road length and building exposure at the primary 500 m resolution.

Exposure Indicator	Spearman ρ with Share of Road Length in Upper Centrality Decile
Exposed buildings	0.614
Exposed building footprint share	0.604
Buildings ≥60 dB	0.591
Building-footprint area ≥60 dB	0.585
Buildings ≥65 dB	0.516
Building-footprint area ≥65 dB	0.515

A further partial rank analysis at local council level accounted for building density and road length density (n = 68; Supplementary Table S6b). For the share of road length in the highest centrality decile, the correlation with the ≥50 dB exposed footprint percentage was ρ = 0.586 before adjustment and 0.635 after adjustment. For absolute ≥60 dB and ≥65 dB exposed footprint areas, the corresponding coefficients were ρ = 0.611 and 0.626 before adjustment and 0.629 and 0.640 after adjustment. These descriptive results show that the positive local council associations were not reduced by the two density controls. They do not establish an independent relationship at grid level and do not account for traffic volumes, receptor conditions or spatial dependence. A separate analysis of the 1260 eligible 500 m cells calculated partial rank correlations after accounting for building count and total filtered road length. For the share of road length in the highest centrality decile and exposed footprint percentage, Spearman's ρ was 0.604 before adjustment and 0.539 after adjustment. For the absolute ≥60 dB footprint area, the coefficients were 0.584 and 0.509. For mean centrality and exposed footprint percentage, the coefficient decreased from 0.383 to 0.360 (Supplementary Tables S12 and S12b). These tests reduce, but do not eliminate, concerns about confounding. Mapped traffic intensity was not included.

4.4. Priority Locations

At 500 m, 23 cells were in the highest decile of mean structural centrality weighted by road length and in the highest decile of ≥60 and/or ≥65 dB exposed building footprint areas. Ten cells satisfied both noise criteria, two additional cells satisfied only the ≥60 dB criterion, and eleven satisfied only the ≥65 dB criterion. Grouping cells that shared an edge or vertex produced 15 spatial clusters. Table S8 identifies each selected cell by its (ix, iy) grid key, local council, component, road length, centrality weighted by road length, total and exposed footprint areas in the higher noise classes, and the two screening flags. Table S9 gives the 15 cluster summaries. An independent recalculation from the 500 m GeoPackage identified the same 23 cells.

The largest clusters followed Triq l-Imdina across Attard and Żebbuġ, Tal-Balal across Iklin, Gharghur and Saint John, and roads around Buqana/Rabat–Mosta, Naxxar–Iklin,

Luqa and Triq tal-Barrani in Għaxaq–Żejtun. Other priority locations were identified in Raħal Ġdid, Msida, Saint Paul's Bay, Mdina and Cospicua and in Gozo near Kerċem and Xewkija. These locations show where structural importance of the network coincides with higher mapped building exposure. They do not demonstrate that centrality causes acoustic exposure. Compared with the 90th percentile threshold, an 85th percentile threshold selected 56 cells, including all original 23. A 92.5th percentile threshold selected eight cells, all belonging to the original set. At the 90th percentile, using the proportion of exposed footprint rather than the absolute higher noise area, 40 cells were selected, including 22 of the original 23. Screening exposure alone in the highest decile selected 152 cells. These results show that a core of cells persists across criteria, while the total number depends on the screening definition (Table S10). The 23 selected cells should therefore not be interpreted as an externally validated ranking of interventions.

4.5. Sensitivity Analysis

The national number of exposed buildings declined progressively as stricter minimum footprint-intersection thresholds were imposed. From the primary value of 13,773 buildings, exposure declined to 13,532 at 1%, 12,917 at 5%, 12,090 at 10%, 10,454 at 25% and 8753 at 50%. Consequently, 87.8% of buildings identified under the primary definition remained classified as exposed when at least 10% of their footprint was required to fall within one noise class.

The ≥70 dB class provided a more stringent test. Its building count declined from 147 under the primary definition to 121, 85, 67, 40 and 22 under the 1%, 5%, 10%, 25% and 50% thresholds, respectively. The persistence of 67 buildings under the 10% criterion and 22 buildings under the 50% criterion shows that the highest-noise intersections are not explained solely by marginal polygon contact.

5. Discussion

Mapped night-time road traffic noise is unevenly distributed across Malta's physical built environment, and national totals conceal differences among building footprints, local councils and transport corridors. The study assesses spatial intersections with statutory Lnight polygons and examines their relationships with aggregate census descriptors and road-network topology. Its first contribution is distinguishing the number of building-footprint features intersected from the area of built fabric affected. Of the 142,681 footprint features, 9.65% intersected the published ≥50 dB contours, whereas intersected footprint areas accounted for 6.26% of the national total. These are complementary geospatial screening measures; neither is a direct acoustic measurement at a façade or a measure of persons exposed. The published bands also do not capture the full range of night-time noise potentially relevant to health, including conditions below the 50 dB mapping threshold.

5.1. Interpretation of Territorial and Socioeconomic Inequalities

The analysis of Malta's local councils reveals a second important distinction: absolute burden and proportional territorial exposure produce different geographical rankings. Saint Paul's Bay and Qormi contained particularly large numbers of affected buildings, while Raħal Ġdid, Mdina, Msida and Marsa recorded high values in relation to the proportion of their building stock intersected. Footprint-area measures produced another partly different geography, with Marsa and Msida particularly prominent.

These differences have direct implications for interpretation. If the policy question concerns the total number of potentially affected buildings, larger local councils may deserve priority. If it concerns the proportion of local built fabric affected, smaller or denser localities may assume greater importance. No exposure indicator, by itself, therefore represents the

full spatial pattern. Population-normalised local council indicators provide additional contextual information but should not, however, be interpreted as person-level exposure rates because building occupancy and within-building population distributions were not modelled.

Extending the analysis to socioeconomic context produced a more nuanced result. The exploratory SDI was only weakly associated with exposure across all local councils, indicating no simple monotonic social gradient at national scale. This is consistent with European evidence showing mixed relationships between socioeconomic position and environmental noise exposure across indicators and places [12].

The absence of a strong continuous gradient does not imply that socioeconomic inequality is spatially irrelevant. The most disadvantaged quintile showed higher median exposure to several of the higher noise indicators, and seven local councils combined upper-quintile disadvantage with upper-quintile ≥60 dB footprint exposure. These concentrations support a distributional environmental inequality interpretation at local council level while falling short of demonstrating that disadvantaged individuals themselves are systematically more exposed.

5.2. Network Structure and Environmental Exposure

The road-network results reveal positive descriptive relationships between mapped building exposure and topological road importance. At 500 m, the strongest bivariate associations occurred for the share of road length in the highest centrality decile, rather than the mean centrality score. This share correlated with the exposed building feature count at $\rho = 0.614$ and the exposed footprint share at $\rho = 0.604$; positive coefficients were also observed for higher-noise thresholds. However, road length, the density of building footprints, and traffic-related conditions may explain part of the observed association.Although supplementary partial-rank analyses account for building counts and road length, they do not adjust for observed traffic conditions or spatial dependence. The analysis therefore does not establish an independent predictive effect of network centrality.

These findings extend previous evidence linking traffic noise to urban form, road-network density and local road configuration [26–29]. The present analysis differs in treating centrality as a topological descriptor rather than as a traffic-flow or acoustic-emission proxy and in relating this descriptor to physical building exposure already encoded in statutory Lnight contours across multiple spatial scales.

These associations should not be interpreted causally. Betweenness centrality describes how road segments occupy shortest-path positions within a network; it does not measure traffic flow, vehicle type, congestion, speed or acoustic emission. The result instead indicates that locations containing substantial concentrations of structurally important roads tend also to contain comparatively greater amounts of mapped built-environment exposure.

The persistence of positive relationships at 250, 500 and 1000 m provides additional support for this interpretation. Coefficients increase with aggregation, which is consistent with the smoothing effect of larger spatial units, but the direction remains stable at all scales. The local council analysis produces the same general relationship, showing that the pattern is visible in both regular-grid and administrative representations.

5.3. Priority Screening and Planning Relevance

Priority-based approaches have previously been used to rank road stretches for noise action planning [52]. In this study, priority areas are identified through the spatial coincidence of upper-decile structural centrality and upper-decile higher-noise building-footprint exposure, rather than through a weighted intervention index applied to individual road stretches.

The priority screening identified 23 cells in the 500 m grid, grouped into 15 clusters by queen contiguity, where high structural centrality coincided with larger areas of building footprint exposed to higher noise classes. Because the selection uses the absolute exposed area, a cell with more built area may be included even when the proportion exposed is not especially high. These cells identify locations for further assessment and do not constitute a validated ranking for intervention. The comparison with alternative percentile thresholds and with exposure percentages (Section 4.4; Table S10) shows that the number and location of selected cells depend on the criteria used. The 23 cells therefore represent one defined screening scenario, not a general ranking. Comparison with official Maltese noise action priorities is still needed to assess policy relevance. Before recommending interventions, local acoustic conditions at receptors, building uses, traffic requirements and official noise action priorities should also be considered.

These locations should not automatically be interpreted as intervention zones. Roads with high structural centrality may perform important connectivity functions, making simple traffic removal impractical or even undesirable. Priority locations instead provide candidate areas for subsequent noise action planning, where detailed traffic, acoustic and land-use information can be used to evaluate mitigation measures appropriate to the local context. For this reason, the analytical framework functions as a first-stage spatial screening tool for selecting priority areas and not as a substitute for detailed traffic-engineering or acoustic assessment.

5.4. Robustness

The sensitivity analysis using minimum footprint intersections shows that the national totals are not determined only by small contacts with the mapped polygons. More than 12,000 building features remained classified as exposed when at least 10% of their footprint intersected a noise class, including 67 features in the ≥70 dB class. This result concerns the definition of geometric exposure. It does not measure uncertainty in the official acoustic model, changes in contour boundaries, building coordinate accuracy or the effects of spatial aggregation. The 10% threshold should not be interpreted as an indicator of noise dose or health risk. A separate overlay audit identified 12.72 m^2 of overlap between noise classes and 38 building features whose total mapped area exceeded their footprint area by a combined 0.0223 m^2. These differences are too small to affect national totals at the reported precision. No buffer or displacement test of the official contours was carried out. Uncertainty in acoustic model inputs and positional accuracy therefore remains outside this audit.

5.5. Limitations

The results describe where building footprints intersect the mapped noise contours. They do not measure noise at façades or individual exposure. A façade assessment would require information on receiver height, orientation, shielding, local acoustic conditions, and building use and occupancy, none of which was modelled here. All building footprints were included, regardless of their use. This is appropriate for analysing the built environment, but the results cannot be used to estimate the number of residents or households exposed at night or associated health effects. The socioeconomic analysis uses local council indicators of education, unemployment and housing conditions, each with a different denominator. It does not include income, differences within local councils or adjustments for demographic composition. These indicators were not assigned to individual buildings or residents. The overlap between disadvantaged local councils and higher mapped exposure does not establish that disadvantaged individuals are themselves exposed [43,44].

The acoustic analysis uses only the published Round-4 major-road Lnight contours at ≥50 dB. The WHO recommends night-time road traffic noise below 45 dB Lnight [1], so

this dataset does not cover all noise levels that may be relevant to health. Locations outside these polygons cannot be assumed to have noise below 50 dB or to be free of road traffic noise. The contours represent modelled noise classes, not measurements at individual façades. Contour boundaries, road-source representation, small polygon artefacts and the position of building footprints can affect intersection counts and noise class assignments. The minimum footprint overlap tests address only part of this geometric uncertainty. We did not test the effects of shifting or buffering the noise contours. Although overlap between noise classes was measured, this does not establish the accuracy of the acoustic model. Verification of façade noise levels and the effects of contour displacement require additional analyses.

Network centrality describes the position of roads within the network and does not measure observed traffic. The graph is undirected and uses road length as cost. It does not take account of turning restrictions, one-way streets, traffic speeds, congestion or vehicle composition. Structural nodes were used as origins rather than all geometry vertices to reduce the effect of road digitisation, and up to 500 origins per larger component were selected using seed 42. Percentiles were calculated separately within components. The sensitivity tests showed that centrality rankings remained relatively stable when sample sizes and random seeds were changed. Using all geometry vertices as origins or replacing component-based percentile normalisation with global ranking resulted in larger differences, especially for roads classified in the highest centrality decile. The main network patterns are therefore relatively stable, but the classification of individual roads is more sensitive to these modelling choices. The comparisons at 250, 500 and 1000 m show how the associations vary with spatial scale, but they do not eliminate spatial autocorrelation, possible confounding or the modifiable areal unit problem. A separate spatial analysis of the 1260 eligible 500 m cells used binary queen adjacency, with 9172 directed neighbour pairs and no isolated cells. Moran's I was 0.351 for the share of road length in the highest centrality decile, 0.311 for the exposed footprint percentage and 0.330 for the absolute ≥60 dB footprint area (999 random label permutations, two-sided $p = 0.001$; Table S15). These results show spatial clustering and support interpreting the correlations as descriptive rather than causal. However, the permutation tests do not correct the reported correlations between centrality and exposure for spatial dependence.

5.6. Implications and Transferability

The integration demonstrates several distinct uses of regulatory mapping. Building-footprint intersections reveal where physical built fabric crosses published noise bands. Comparisons among local councils identify localities where high mapped exposure co-occurs with area-level socioeconomic disadvantage. Separately, centrality-exposure maps identify corridors where mapped higher-noise building exposure and structurally important road segments occur together. The present study does not establish a three-way coincidence of disadvantage, acoustic exposure and centrality at a common unit nor does it estimate individual risk. Both screening approaches can help direct more detailed façade-level acoustic, transport and social assessments.

The analytical framework is transferable to other territories covered by strategic noise mapping, provided that comparable data on road noise, buildings and road networks are available. Applying the same workflow to successive strategic noise-mapping cycles produced under Directive 2002/49/EC may allow consistent comparison of spatial changes in the relationship between built-environment exposure and road-network structure.

6. Conclusions

This study developed a reproducible geospatial framework for analysing night-time road traffic noise in Malta's built environment. It combines Lnight contours from the 2021 fourth cycle of strategic noise mapping, national building footprints, local council boundaries and structural road-network centrality.

Of the 142,681 building footprints analysed, 13,773 (9.65%) intersected at least one published Lnight contour ≥50 dB. The corresponding intersected footprint area was approximately 1.92 km^2, or 6.26% of Malta's total building-footprint area. Fewer buildings intersected the higher noise classes: 3973 buildings (2.78%) reached a maximum intersected class of at least 60 dB, 1451 (1.02%) reached at least 65 dB and 147 intersected the ≥70 dB class. The distribution also varied among local councils. Those with the largest number of affected buildings were not necessarily those with the highest proportion of buildings or footprint area exposed. The socioeconomic analysis did not show a strong monotonic relationship across all local councils. However, the most disadvantaged quintile had higher median exposure for several higher noise indicators, and seven councils combined upper-quintile disadvantage with upper-quintile ≥60 dB footprint exposure.

Road network analysis provided another dimension for interpreting these spatial patterns. At 500 m, the share of road length in the highest centrality decile was positively associated with the exposed building count ($\rho = 0.614$) and exposed footprint share ($\rho = 0.604$); the sign also remained positive at 250 and 1000 m. The priority screening identified 23 cells in the 500 m grid, grouped into 15 clusters, where high mean structural centrality coincided with greater absolute building-footprint area in the ≥60 and/or ≥65 dB classes. The main correlations are descriptive and unadjusted. Additional partial rank tests accounted for building counts and road length but not traffic activity or spatial dependence. The selected cells depend on the screening criteria and should not be interpreted as a validated ranking for intervention.

These locations show spatial overlap, not a causal relationship. Structural centrality cannot replace traffic or acoustic modelling. It provides additional information on the position of roads in the network when interpreting mapped noise exposure. The sensitivity analysis also shows that the main exposure results are not explained only by small intersections with noise contours: 12,090 buildings remained classified as exposed under a 10% minimum footprint criterion.

The contribution of this study is to combine official noise contours, building footprints, socioeconomic indicators and road-network centrality in a spatial screening of Malta. The analysis identifies two different spatial patterns: local councils where higher mapped exposure coincides with socioeconomic disadvantage and corridors where greater building-footprint exposure coincides with structurally important roads. These results should be considered separately. They do not demonstrate individual environmental inequality or a causal relationship between socioeconomic disadvantage, network centrality and noise exposure. The results can help identify where more detailed studies are needed. Decisions on noise mitigation will still require information on façade noise levels, traffic conditions, building use and the population affected.

Supplementary Materials: The following supporting information can be downloaded at: https://www.mdpi.com/article/10.3390/geographies6040117/s1. Figure S1: Locations and identifiers of the 23 priority 500 m cells; Table S1: Standardisation parameters for the socioeconomic disadvantage index (SDI); Table S2: SDI and component Spearman correlations with exposure indicators; Table S3: Intercorrelations among SDI components; Table S4: Complete socioeconomic and exposure indicators for the 68 local councils; Table S5: Exploratory Moran's I at local council level; Table S6a: Local council road and building density inputs; Table S6b: Exploratory local council partial-rank correlations; Table S7: Original multiscale correlations and sample sizes; Table S8: Full audit of the 23 priority

cells; Table S9: Full audit of the 15 priority clusters; Table S10: Sensitivity of priority selection to thresholds and proportional exposure; Table S11: Reconstructed 1000 m grid from the 500 m data; Table S12: Grid partial-rank correlations adjusted for building count and road length; Table S12b: Centrality-share adjusted correlations at 500 m; Table S13: Gridded sample sizes; Table S14: Zero values and tied ranks in the 500 m grid; Table S15: Spatial autocorrelation in the 500 m grid.

Author Contributions: Conceptualization, R.M.C. and M.V.B.; methodology, R.M.C. and J.R.; software, R.M.C.; formal analysis, R.M.C.; investigation, R.M.C.; data curation, R.M.C.; validation, R.M.C.; visualization, R.M.C.; writing—original draft preparation, R.M.C.; writing—review and editing, R.M.C., J.R. and M.V.B. All authors have read and agreed to the published version of the manuscript.

Funding: This research was funded by the European Union under the Horizon Europe Programme, Grant Agreement No. 101217375 (GREEN TALENT). The views and opinions expressed are, however, those of the author(s) only and do not necessarily reflect those of the European Union or the granting authority. Neither the European Union nor the granting authority can be held responsible for them.

Institutional Review Board Statement: Not applicable.

Informed Consent Statement: Not applicable.

Data Availability Statement: The original contributions presented in this study are included in the article/Supplementary Material. Further inquiries can be directed to the corresponding author.

Acknowledgments: During the preparation of this manuscript, the authors used OpenAI ChatGPT (web service; no fixed version reported; https://chatgpt.com/; accessed on 2 November 2026) for language editing, assistance with code development, and manuscript preparation. The authors reviewed and edited all outputs and take full responsibility for the content of this publication.

Conflicts of Interest: Ricardo Mendes Correia and Mario V. Balzan were employed by the company EcoStack Innovations Limited. The remaining author declares that the research was conducted in the absence of any commercial or financial relationships that could be construed as a potential conflict of interest.

References

1. World Health Organization Regional Office for Europe. *Environmental Noise Guidelines for the European Region*; WHO Regional Office for Europe: Copenhagen, Denmark, 2018.
2. European Environment Agency (EEA). *Environmental Noise in Europe 2025*; EEA Report 05/2025; Publications Office of the European Union: Luxembourg, 2025. Available online: https://www.eea.europa.eu/en/analysis/publications/environmental-noise-in-europe-2025 (accessed on 2 November 2026).
3. European Parliament and Council. Directive 2002/49/EC of the European Parliament and of the Council of 25 June 2002 relating to the assessment and management of environmental noise. *Off. J. Eur. Communities* **2002**, *L189*, 12–25.
4. Kephalopoulos, S.; Paviotti, M.; Anfosso-Lédée, F. *EUR 25379 EN*; Common Noise Assessment Methods in Europe (CNOSSOS-EU); Publications Office of the European Union: Luxembourg, 2012.
5. Kephalopoulos, S.; Paviotti, M.; Anfosso-Lédée, F.; Van Maercke, D.; Shilton, S.; Jones, N. Advances in the development of common noise assessment methods in Europe: The CNOSSOS-EU framework for strategic environmental noise mapping. *Sci. Total Environ.* **2014**, *482–483*, 400–410. [CrossRef] [PubMed]
6. Longley, P.A.; Goodchild, M.F.; Maguire, D.J.; Rhind, D.W. *Geographic Information Systems and Science*, 2nd ed.; John Wiley and Sons: Hoboken, NJ, USA, 2005.
7. Ko, J.H.; Chang, S.I.; Lee, B.C. Noise impact assessment by utilizing noise map and GIS: A case study in the city of Chungju, Republic of Korea. *Appl. Acoust.* **2011**, *72*, 544–550. [CrossRef]
8. Seong, J.C.; Park, T.H.; Ko, J.H.; Chang, S.I.; Kim, M.; Holt, J.B.; Mehdi, M.R. Modeling of road traffic noise and estimated human exposure in Fulton County, Georgia, USA. *Environ. Int.* **2011**, *37*, 1336–1341. [CrossRef] [PubMed]
9. Khan, J.; Ketzel, M.; Kakosimos, K.; Sørensen, M.; Jensen, S.S. Road traffic air and noise pollution exposure assessment—A review of tools and techniques. *Sci. Total Environ.* **2018**, *634*, 661–676. [CrossRef] [PubMed]
10. Puyana-Romero, V.; Cueto, J.L.; Gey, R. A 3D GIS tool for the detection of noise hot-spots from major roads. *Transp. Res. Part D Transp. Environ.* **2020**, *84*, 102376. [CrossRef]
11. Baclet, S.; Venkataraman, S.; Rumpler, R.; Billsjö, R.; Horvath, J.; Österlund, P.E. From strategic noise maps to receiver-centric noise exposure sensitivity mapping. *Transp. Res. Part D Transp. Environ.* **2022**, *102*, 103114. [CrossRef]

12. Dreger, S.; Schüle, S.A.; Hilz, L.K.; Bolte, G. Social inequalities in environmental noise exposure: A review of evidence in the WHO European Region. *Int. J. Environ. Res. Public Health* **2019**, *16*, 1011. [CrossRef] [PubMed]
13. Newman, M.E.J. *Networks: An Introduction*; Oxford University Press: Oxford, UK, 2010. [CrossRef]
14. Freeman, L.C. A set of measures of centrality based on betweenness. *Sociometry* **1977**, *40*, 35–41. [CrossRef]
15. Freeman, L.C. Centrality in social networks: Conceptual clarification. *Soc. Netw.* **1978**, *1*, 215–239. [CrossRef]
16. Crucitti, P.; Latora, V.; Porta, S. Centrality in networks of urban streets. *Chaos* **2006**, *16*, 015113. [CrossRef] [PubMed]
17. Porta, S.; Crucitti, P.; Latora, V. The network analysis of urban streets: A primal approach. *Environ. Plan. B Plan. Des.* **2006**, *33*, 705–725. [CrossRef]
18. Sevtsuk, A.; Mekonnen, M. Urban network analysis: A new toolbox for ArcGIS. *Rev. Int. De Géomatique* **2012**, *22*, 287–305. [CrossRef]
19. Porta, S.; Strano, E.; Iacoviello, V.; Messora, R.; Latora, V.; Cardillo, A.; Wang, F.; Scellato, S. Street centrality and densities of retail and services in Bologna, Italy. *Environ. Plan. B Plan. Des.* **2009**, *36*, 450–465. [CrossRef]
20. Porta, S.; Latora, V.; Wang, F.; Rueda, S.; Strano, E.; Scellato, S.; Cardillo, A.; Belli, E.; Cárdenas, F.; Cormenzana, B.; et al. Street centrality and the location of economic activities in Barcelona. *Urban Stud.* **2012**, *49*, 1471–1488. [CrossRef]
21. Rui, Y.; Ban, Y. Exploring the relationship between street centrality and land use in Stockholm. *Int. J. Geogr. Inf. Sci.* **2014**, *28*, 1425–1438. [CrossRef]
22. Correia, R.M.; Guerreiro, M.R.; Brandão, F.J.S. Data-driven spatial analysis of urban renewal: Network kernel density estimation of building renovation. In *Formal Methods in Architecture*; Eloy, S., Leite Viana, D., Morais, F., Vieira Vaz, J., Eds.; Springer: Berlin/Heidelberg, Germany, 2021; pp. 185–195. [CrossRef]
23. Rubulotta, E.; Ignaccolo, M.; Inturri, G.; Rofè, Y. Accessibility and centrality for sustainable mobility: Regional planning case study. *J. Urban Plan. Dev.* **2013**, *139*, 115–132. [CrossRef]
24. Correia, R.M. Sistemas De Informação Geográfica Na Avaliação De Fenómenos Urbanos Emergentes: O Papel Do Airbnb No Crescimento Da Reabilitação Urbana Em Lisboa (2015–2019). Ph.D. Thesis, Iscte—Instituto Universitário de Lisboa, Lisboa, Portugal, 2024.
25. Correia, R.M.; Rocha, J. Platform Urbanism and Spatial Centrality in Short-Term Rental Research: A Kernel-Density Framework for Planning Analytics. Centre for Research in Anthropology (CRIA), Iscte—Instituto Universitário de Lisboa, Lisbon, Portugal (R.M.C.); Institute of Geography and Spatial Planning (IGOT), Universidade de Lisboa, Lisbon, Portugal (J.R.). 2026; *manuscript in preparation*.
26. Salomons, E.M.; Berghauser Pont, M. Urban traffic noise and the relation to urban density, form, and traffic elasticity. *Landsc. Urban Plan.* **2012**, *108*, 2–16. [CrossRef]
27. Ryu, H.; Park, I.K.; Chun, B.S.; Chang, S.I. Spatial statistical analysis of the effects of urban form indicators on road traffic noise exposure of a city in South Korea. *Appl. Acoust.* **2017**, *115*, 93–100. [CrossRef]
28. Lu, X.; Kang, J.; Zhu, P.; Cai, J.; Guo, F.; Zhang, Y. Influence of urban road characteristics on traffic noise. *Transp. Res. Part D Transp. Environ.* **2019**, *75*, 136–155. [CrossRef]
29. Asgarian, A. Street network configuration and traffic noise patterns: A GAM-based analysis of spatial associations in Jiroft, Iran. *Environ. Monit. Assess.* **2026**, *198*, 809. [CrossRef] [PubMed]
30. Vogiatzis, C.; Vasiliadis, V. Environmental noise investigation procedure in the urban road network in Malta. In Proceedings of the 14th International Congress on Sound and Vibration, Cairns, Australia, 9–12 July 2007; Australian Acoustical Society: Magill North, SA, Australia, 2007; pp. 3390–3397.
31. Jones, M.C. Noise Pollution: A Case Study of Mriehel By-Pass, Qormi Malta. Bachelor's Thesis, University of Malta, Msida, Malta, 2008.
32. Camilleri, C. A noise pollution study of the Maltese Islands. Master's Thesis, University of Malta, Msida, Malta, 2009.
33. Buhagiar, V.; Giglio, F. *Noise and Vibration Studies for the Environmental Planning Statement and Appropriate Assessment Required for the Kappara Junction Project*; EcoServ & CADA: Mosta, Malta, 2012.
34. Environment and Resources Authority (ERA). *Final Project Report: Round 4 Strategic Noise Mapping: Provision of Consultancy Services for Round 4 Reporting Obligations Including the Strategic Noise Mapping in Malta Under Directive 2002/49/EC*; ERA: Mosta, Malta, 2024.
35. European Environment Agency (EEA). *Noise Contours Data Reported Under Environmental Noise Directive (END) 2022 (Vector), March 2026*; EEA Datahub: Copenhagen, Denmark, 2026.
36. Planning Authority. *Large Scale Topography Buildings*; Malta Data Portal: Valletta, Malta, 2026.
37. Planning Authority. *Local Councils Units and Boundaries*; Malta Data Portal: Valletta, Malta, 2026.
38. National Statistics Office Malta. *Census of Population and Housing 2021: Final Report: Population, Migration and Other Social Characteristics*; NSO Malta: Valletta, Malta, 2023; Volume 1.
39. National Statistics Office Malta. *Census of Population and Housing 2021: Final Report: Dwelling Characteristics*; NSO Malta: Valletta, Malta, 2023; Volume 2.

40. National Statistics Office Malta. *Census of Population and Housing 2021: Final Report: Health, Education, Employment and Other Characteristics*; NSO Malta: Valletta, Malta, 2024; Volume 3.
41. Geofabrik GmbH. *Malta OpenStreetMap Data Extracts: Historical Shapefile Extract, January 2022*; Geofabrik GmbH: Karlsruhe, Germany, 2022.
42. OpenStreetMap contributors. *OpenStreetMap Data: Malta*; Open Database Licence: London, UK, 2022.
43. Robinson, W.S. Ecological correlations and the behavior of individuals. *Am. Sociol. Rev.* **1950**, *15*, 351–357. [CrossRef]
44. Wakefield, J. Ecologic studies revisited. *Annu. Rev. Public Health* **2008**, *29*, 75–90. [CrossRef] [PubMed]
45. Brandes, U. A faster algorithm for betweenness centrality. *J. Math. Sociol.* **2001**, *25*, 163–177. [CrossRef]
46. Hagberg, A.A.; Schult, D.A.; Swart, P.J. Exploring network structure, dynamics, and function using NetworkX. In *Proceedings of the 7th Python in Science Conference, Pasadena, CA, USA, August 2008*; SciPy: Pasadena, CA, USA, 2008; pp. 11–15. [CrossRef]
47. Openshaw, S. The Modifiable Areal Unit Problem. In *Concepts and Techniques in Modern Geography*; Geo Books: Hong Kong, China, 1983; Volume 38.
48. Anselin, L. *Spatial Econometrics: Methods and Models*; Kluwer Academic Publishers: Dordrecht, The Netherlands, 1988. [CrossRef]
49. QGIS Development Team. *QGIS Geographic Information System*; QGIS Association: Laax, Switzerland, 2026.
50. Fisher, W.D. On grouping for maximum homogeneity. *J. Am. Stat. Assoc.* **1958**, *53*, 789–798. [CrossRef]
51. Jenks, G.F.; Caspall, F.C. Error on choroplethic maps: Definition, measurement, reduction. *Ann. Assoc. Am. Geogr.* **1971**, *61*, 217–244. [CrossRef]
52. Ruiz-Padillo, A.; Torija, A.J.; Ramos-Ridao, A.; Ruiz, D.P. A methodology for classification by priority for action: Selecting road stretches for network noise action plans. *Transp. Res. Part D Transp. Environ.* **2014**, *29*, 66–78. [CrossRef]

Disclaimer/Publisher's Note: The statements, opinions and data contained in all publications are solely those of the individual author(s) and contributor(s) and not of MDPI and/or the editor(s). MDPI and/or the editor(s) disclaim responsibility for any injury to people or property resulting from any ideas, methods, instructions or products referred to in the content.